

# Dynamics of the Neoproterozoic carbon cycle

Daniel H. Rothman<sup>\*†</sup>, John M. Hayes<sup>‡</sup>, and Roger E. Summons<sup>\*</sup>

<sup>\*</sup>Department of Earth, Atmospheric, and Planetary Sciences  
Massachusetts Institute of Technology  
Cambridge, MA 02139

<sup>‡</sup>Department of Geology and Geophysics  
Woods Hole Oceanographic Institution  
Woods Hole, MA 02543

May 9, 2003

To appear in *Proc. Natl. Acad. Sci. USA*

## ABSTRACT

The existence of unusually large fluctuations in the Neoproterozoic (1000–543 Ma) carbon-isotopic record implies strong perturbations to the Earth’s carbon cycle. To analyze these fluctuations, we examine records of both the isotopic content of carbonate carbon and the fractionation between carbonate and marine organic carbon. Together, these are inconsistent with conventional, steady-state models of the carbon cycle. The records can, however, be well understood as deriving from the non-steady dynamics of two reactive pools of carbon. The lack of a steady state is traced to an unusually large oceanic reservoir of organic carbon. We suggest that the most significant of the Neoproterozoic negative carbon-isotopic excursions resulted from increased remineralization of this reservoir. The terminal event, at the Proterozoic-Cambrian boundary, signals the reservoir’s final diminution, a process which was likely initiated by evolutionary innovations that increased export of organic matter to the deep sea.

---

<sup>†</sup>To whom correspondence should be addressed. Email: [dan@segovia.mit.edu](mailto:dan@segovia.mit.edu)

The co-evolution of the biosphere and geosphere is reflected in large part by changes in the long-term carbon cycle [1]. Past changes within the cycle are recorded in the isotopic content of carbonate and organic carbon buried in ancient sediments [2]. Extraordinarily large fluctuations occur in the Neoproterozoic (1000–543 Ma) carbon-isotopic record, both immediately preceding the Cambrian diversification of complex animal life [3–5] and in the roughly 200 My before it [6]. There is much interest in determining not only the cause of these isotopic events [3–9] but how, if at all, they are related to early animal evolution [10].

Here we analyze a significant portion of the Neoproterozoic isotopic record by portraying it as a dynamical trajectory in a two-dimensional space indexed by the isotopic content of carbonate carbon and the fractionation between carbonate and marine organic carbon. This depiction, analogous to the construction of phase portraits in dynamical systems theory [11], provides specific predictions for a carbon cycle evolving quasi-statically in a succession of steady states. We find that the Cenozoic portion (0–65 Ma) of the carbon-isotopic record satisfies these predictions. However the Neoproterozoic record does not.

The dynamics of a system with two sizeable and isotopically distinct pools of reactive carbon suffice to explain the Neoproterozoic records. Then as now one pool was oceanic and atmospheric  $\text{CO}_2$ . Here we show that the other was probably oceanic organic carbon. The isotopic data indicate that this reservoir was large and that its average properties changed slowly. However, fluctuations in its size would have led to major variations in the isotopic record. Moreover, even if the size of the organic reservoir had been perfectly constant, changes in the fractionation associated with organic production would have led to isotopic fluctuations much greater than those predicted by steady-state theory.

The fluctuations of greatest interest are those associated with large-scale glaciations [8, 9] and with the end of the Proterozoic. Large glaciations would have led to enhanced remineralization of marine organic carbon and thus to decreases in the  $^{13}\text{C}$  content of carbonates. A final diminution of the organic reservoir in the latest Neoproterozoic would have had a similar effect. The terminal event was probably induced by enhanced biomineralization, production of resistant biopolymers, and the invention of fecal pellets by early metazoans, each of which acted to sweep organic carbon from ocean waters.

Each of these conclusions is predicated on our phase-plane analysis, to which we now proceed.

## Phase Portraits

We first consider the oceans as a single reservoir of a mass  $m$  of carbon, with an incoming flux  $j_i$  and an outgoing (burial) flux  $j_{\text{out}}$ . The isotopic composition<sup>§</sup>  $\delta$  of

---

<sup>§</sup>From isotopic abundance ratios  $R = (^{13}\text{C}/^{12}\text{C})$ , the isotopic composition  $\delta$  is given by  $\delta = 1000[(R - R_{\text{STD}})/R_{\text{STD}}]$ , where  $R_{\text{STD}}$  is the abundance ratio for a standard sample.

oceanic carbon then changes as [12]

$$\frac{d\delta}{dt} = \frac{1}{m} \left( j_i(\delta_i - \delta) - j_{\text{out}}(\delta_{\text{out}} - \delta) \right), \quad (1)$$

where  $\delta_i$  is the isotopic composition of incoming carbon,  $\delta_{\text{out}}$  is the isotopic composition of outgoing carbon in all forms, and  $m$  changes according to  $dm/dt = j_i - j_{\text{out}}$ . The output occurs as carbonate or organic carbon with isotopic composition  $\delta_a \simeq \delta$  and  $\delta_o = \delta_a - \varepsilon$ , respectively. The fractionation  $\varepsilon > 0$  results from isotope effects associated with carbonate equilibria and photosynthetic carbon fixation. Assuming that the organic portion of the output is a fraction  $f$  (typically about 0.2–0.3 [13,14]) of the total, equation (1) yields

$$\frac{d\delta_a}{dt} = \frac{1}{m} \left( j_i(\delta_i - \delta_a) + f j_{\text{out}} \varepsilon \right). \quad (2)$$

In steady state,  $j_i = j_{\text{out}} \equiv j^*$  and the right-hand side above vanishes. Denoting all steady-state quantities with asterisks, we obtain

$$\delta_a^* = \delta_i + f\varepsilon^*. \quad (3)$$

This relation is typically assumed valid at time scales greater than  $\tau = m^*/j^*$  (about  $10^5$  yr presently [1, 14]), i.e., for a carbon cycle evolving quasi-statically from one steady state to another. In such cases equation (3) is commonly employed to estimate the organic burial fraction  $f$  when  $\delta_a$  and  $\varepsilon = \delta_a - \delta_o$  are known [1, 15]. To do so,  $\delta_i$  is typically set equal to the average isotopic composition of all crustal carbon [1, 15], about  $-5\text{‰}$  [14].

We consider instead an alternative method for the estimation of  $f$ . Specifically we assume only that  $\delta_i$  and  $f$  change more slowly than  $\delta_a$  and  $\varepsilon$ , which vary quasi-statically such that equation (3) holds. Plots of  $\delta_a$  vs.  $\varepsilon$  will then describe a straight line whose slope  $\hat{f}$  and intercept  $\hat{\delta}_i$  are estimates of  $f$  and  $\delta_i$ . In analogy with the theory of dynamical systems, we consider such plots to be phase portraits and seek geometric depictions of dynamical attractors [11]. The line described by equation (3) is but one (trivial) example, corresponding to a sequence of steady states.

The straight line in Figure 1a shows that the assumption of quasi-static evolution with constant  $f$  and  $\delta_i$  is reasonable for the Cenozoic. The line's slope,  $\hat{f} \simeq 0.30$ , and intercept,  $\hat{\delta}_i \simeq -6.1\text{‰}$ , are close to values typical of  $f$  and  $\delta_i$  for the Phanerozoic [13, 14]. Figure 1b displays similar results for the latest Precambrian and early Cambrian, yielding  $\hat{f} \simeq 0.29$  and  $\hat{\delta}_i \simeq -8.7\text{‰}$ .

Figure 2, however, shows far different results for Neoproterozoic records ranging from about 738 Ma to 555 Ma. The data are displayed four ways, two of which depend on time (2a and 2b), and two of which do not (2c and 2d). As shown in Figures 2c and 2d, we find again a straight-line relationship, but now with  $\hat{f} \simeq 1.0$  and  $\hat{\delta}_i \simeq -24\text{‰}$ , values which are, respectively, extraordinarily high and low. Of equal interest is the time-ordered depiction of the data in Figure 2b, where the isotopic excursions are

portrayed as a dynamical trajectory in the phase plane defined by  $\varepsilon$  and  $\delta_a$ . Except for a brief interlude around 590 Ma, the data lie on a remarkably stable attractor. Figure 2d, which plots only values of  $\delta_a$  and  $\varepsilon$  derived from the same sample (i.e., those for which correlations between strata in different rock units are not required), confirms that the extreme values of  $\hat{f}$  and  $\hat{\delta}_i$  are dependent neither on global averaging nor temporal correlation.

The phase portraits of Figure 2 therefore unambiguously indicate an unusual dynamical state. We next consider its possible causes.

## The Neoproterozoic Attractor

How could  $\hat{f} \simeq 1.0$  and  $\hat{\delta}_i \simeq -24\%$ ? We consider four hypotheses: *i*) the Neoproterozoic carbon cycle existed in an extreme state in which inputs and outputs were nearly entirely organic in origin; *ii*) correlations between  $f$  and  $\varepsilon$  or  $f$  and  $\delta_i$  mask less extreme, time-dependent values of  $f$  and  $\delta_i$ ; *iii*) the results derive from spurious correlations between  $\delta_a$  and  $\delta_a - \delta_o$ ; and *iv*) the assumption of quasi-static evolution is invalid.

Acceptance of the first hypothesis requires either the virtual absence of carbonate sedimentation or, assuming carbonate deposition rates similar to the Phanerozoic, burial of organic carbon at rates ten-fold those in the Phanerozoic. The former possibility is eliminated by the abundance of carbonates in the Neoproterozoic record [15]. The latter requires huge fluxes of organic matter and nutrients *and* the subsequent deletion of evidence of these processes from the record, presumably by subduction. This combination is highly improbable. Equally fortuitous would be the second hypothesis: correlations between geochemical variables that conspire to drive  $\hat{f}$  not only upwards, but all the way to and no further than unity.

The third hypothesis can be rejected quantitatively. If  $\delta_a$  and  $\delta_o$  contained no signal but were instead independent random variables with equal variance, plots of  $\delta_a$  vs.  $\varepsilon = \delta_a - \delta_o$  would yield a slope—the reduced major axis [16]—of  $(\text{var } \delta_a / \text{var } \varepsilon)^{1/2} = 1/\sqrt{2} \simeq 0.71$ , well outside the 95% confidence intervals for  $\hat{f}$  (see caption, Figure 2).

The fourth hypothesis—the lack of a steady state—would appear unattractive given that, on average, the data do not resolve time scales less than about 5 My, or about fifty carbon-residence times in the modern oceans [1, 14]. Note, however, that  $\hat{f} \simeq 1.0$  is equivalent to the observation that  $\delta_o \simeq \text{const.}$ , which may be inferred immediately from Figure 2a or noted directly from Figure 1 of Ref. [15]. If only  $\delta_a$  responded to contemporary processes while  $\delta_o$  remained invariant due to background recycling of ancient organic material, the data would require the unlikely onset and cessation of that condition simultaneously in multiple sedimentary basins. We therefore seek generic mechanisms that force  $\delta_o$  to vary slowly while allowing  $\delta_a$  to change substantially. Slow variation of  $\delta_o$  implies a large pre-depositional reservoir of organic carbon which equilibrates slowly with respect to any changes in its inputs or outputs. Provided this equilibration time is slow enough, any such changes will be dynamic

rather than quasi-static. The possibility of non-steady state dynamics therefore deserves further attention.

## Theory

Figure 3 provides a model. The oceans' inventory of carbon is partitioned into reservoirs of inorganic and organic carbon, with isotopic compositions  $\delta_1$  and  $\delta_2$  and residence times  $\tau_1$  and  $\tau_2$ , respectively. The flux from the first to the second reservoir, denoted by  $j_{12}$ , represents organic production; it is isotopically depleted relative to  $\delta_1$  by an amount  $\varepsilon_0$ . The return flux, denoted by  $j_{21}$ , represents remineralization, with no isotopic fractionation. We identify  $\delta_a = \delta_1$  and  $\delta_o = \delta_2$ . However, we do *not* identify  $\varepsilon_0$  with  $\varepsilon = \delta_a - \delta_o$ . The latter quantity is merely an estimate of  $\varepsilon_0$  derived from analyses of buried sediment; only in the case of a steady state will the two be equal in general.

The observation that  $\delta_o = \delta_2$  varies slowly implies that  $\tau_1/\tau_2 \ll 1$ , meaning that the residence time for organic carbon is much longer than that for inorganic carbon. Variations within the carbon cycle correspond to either changes in the fluxes or changes in the isotopic compositions that the fluxes carry. An example of the former is an increase in the remineralization flux, i.e., an increase in the rate of oxidation of reservoir 2. An example of the latter is a decrease in  $\varepsilon_0$  due, e.g., to decreased CO<sub>2</sub> levels or increased algal growth rates [15]. An example of both changes is increased erosion of organic-rich strata. If any of these changes occur at a time scale slower than  $\tau_1$  but faster than  $\tau_2$ ,  $\delta_1$  will decrease while  $\delta_2$  remains relatively constant. The difference

$$\varepsilon = \delta_1 - \delta_2 \tag{4}$$

$$\simeq \delta_1 - \text{const.} \tag{5}$$

will almost precisely track  $\delta_a = \delta_1$ , yielding a slope  $\hat{f} \simeq 1$  in the  $\varepsilon, \delta_a$  phase plane, independent of the real burial fraction  $f$ . The resulting line will intercept the  $\delta_a$ -axis at  $\hat{\delta}_i \simeq -24\text{‰}$  because the steeply sloping trajectories must still pass through the steady solution  $\varepsilon^*, \delta_a^*$  that would occur in the absence of any changes. Slopes  $\hat{f} > 1$  are also possible. For example, organic production following increased remineralization at time scales somewhat slower than  $\tau_2$  would cause  $\delta_o$  to decrease slowly. Consequently  $\varepsilon = \delta_a - \delta_o$  would decrease less than  $\delta_a$ , yielding  $\hat{f} > 1$ .

These effects can be accompanied by large fluctuations in  $\delta_a$ . In the case of an increased remineralization flux, the resulting negative excursion is limited only by the change in the remineralization flux itself, and could in principle approach  $\delta_o \simeq -24\text{‰}$ . Thus  $\delta_a$  is not constrained to be greater than  $\delta_i \simeq -5\text{‰}$ , as in steady-state models. Moreover such large changes need not be accompanied by changes in  $\varepsilon_0$ , even though  $\varepsilon = \delta_a - \delta_o$  will vary with  $\delta_a$ . However changes in  $\varepsilon_0$  are still interesting. In this case  $\delta_a$  will rise and fall with  $\varepsilon_0$ . Comparing equation (5) with (3), we see that when

such non-steady changes in  $\delta_a$  are considered as a function of  $\varepsilon$ , they are a factor of  $1/f \simeq 4$  greater than typical (i.e., Phanerozoic) quasi-static fluctuations.

A formal analysis reveals that the dynamic effects can persist at time scales much longer than  $\tau_2$ . The isotopic compositions and reservoir sizes in Figure 3 evolve as

$$\frac{d\delta_1}{dt} = \frac{j_i}{m_1}(\delta_i - \delta_1) + \frac{j_{21}}{m_1}(\delta_2 - \delta_1) + \frac{j_{12}}{m_1}\varepsilon_0 \quad (6)$$

$$\frac{d\delta_2}{dt} = \frac{j_{12}}{m_2}(\delta_1 - \varepsilon_0 - \delta_2) \quad (7)$$

$$\frac{dm_1}{dt} = j_i + j_{21} - j_{12} - b_1 \quad (8)$$

$$\frac{dm_2}{dt} = j_{12} - j_{21} - b_2, \quad (9)$$

where  $b_1$  and  $b_2$  denote burial fluxes for inorganic and organic carbon, respectively, and, as in equation (1), carbon input to the system is denoted by the flux  $j_i$  with isotopic composition  $\delta_i$ . All fluxes are in general time-dependent.

To characterize non-steady dynamics, we must first obtain the steady solution. The steady state is again given by equation (3), but now augmented by relations equating the total input and output fluxes to and from each reservoir. For reservoir 1 we set this flux equal to  $J_1$ ; i.e.,  $J_1 \equiv j_i + j_{21} = b_1 + j_{12}$ . Likewise, for reservoir 2 we have  $J_2 \equiv b_2 + j_{21} = j_{12}$ . We assume that the characteristic residence times in reservoirs 1 and 2 are  $\tau_1$  and  $\tau_2$ , respectively, yielding steady-state reservoir sizes  $m_1^* = J_1\tau_1$  and  $m_2^* = J_2\tau_2$ .

Relaxation to the steady state occurs at time scales given by the inverse of the eigenvalues  $\lambda_1$  and  $\lambda_2$  of the Jacobian matrix  $\partial\dot{\delta}_j/\partial\delta_k$  evaluated at the steady solution:

$$\frac{\partial\dot{\delta}_j}{\partial\delta_k} = \begin{bmatrix} -J_1/m_1^* & j_{21}/m_1^* \\ j_{12}/m_2^* & -j_{12}/m_2^* \end{bmatrix} = \frac{1}{\tau_1} \begin{bmatrix} -1 & \phi_{21} \\ \mu & -\mu \end{bmatrix}, \quad (10)$$

where

$$\mu = \tau_1/\tau_2 \quad \text{and} \quad \phi_{21} = j_{21}/J_1. \quad (11)$$

To first order in  $\mu$ , assuming  $\mu \ll 1$ , one finds the eigenvalues

$$\lambda_1 \simeq -(1 + \phi_{21}\mu)/\tau_1 \quad (12)$$

$$\lambda_2 \simeq -\mu(1 - \phi_{21})/\tau_1. \quad (13)$$

The first eigenvalue corresponds to a time scale of order  $\tau_1$ . However the slower time scale derived from the second eigenvalue is  $\tau_2/(1 - \phi_{21})$ , which, as  $\phi_{21} \rightarrow 1$ , implies a system-wide relaxation time potentially much longer than  $\tau_2$ .

Whether the system as a whole will indeed require such a long equilibration time will depend on the particular way in which it is perturbed. Specifically, perturbations parallel to the eigenvector  $\mathbf{v}_1$  associated with  $\lambda_1$  decay like  $e^{\lambda_1 t}$ , while perturbations with a significant component parallel to the eigenvector  $\mathbf{v}_2$  associated with  $\lambda_2$  decay

like  $e^{\lambda_2 t}$ . To first order in  $\mu$ ,  $\mathbf{v}_1 \simeq [1, -\mu]$  and  $\mathbf{v}_2 \simeq [\phi_{21} + (\phi_{21} - \phi_{21}^2)\mu, 1]$ . In the limit  $\mu \rightarrow 0$ ,  $\mathbf{v}_1$  corresponds to changes in  $\delta_a$  but not  $\delta_o$ , while  $\mathbf{v}_2$  corresponds to changes in both. Consequently changes in  $\varepsilon_0$ , which affect both  $\delta_a$  and  $\delta_o$ , will indeed require relaxation times on the order of  $1/|\lambda_2|$ . However direct perturbations of  $\delta_a$ , such as those that result from an enhanced remineralization flux  $j_{21}$ , will appear to relax more quickly. In such cases, numerical integrations of the system (6)–(9), discussed further below, indicate an effective system-wide relaxation time roughly equal to  $\tau_2$ .

## Time Scales and Reservoir Sizes

The various time scales can be estimated. In the modern, pre-anthropogenic carbon cycle,  $(1 - \phi_{21}) \simeq 10^{-2}$  and  $\tau_1 \simeq 10^3$  yr [14]. Accepting these as boundaries, the slowest relaxation time scale in the Neoproterozoic,  $\tau_s \equiv 1/|\lambda_2|$ , is

$$\tau_s = \frac{\tau_1}{(1 - \phi_{21})\mu} \gtrsim 10^6 \text{ yr}, \quad (14)$$

where the inequality derives from the assumption that  $\mu \lesssim 10^{-1}$ . The lower bound (14) is conservative: Neoproterozoic  $\text{CO}_2$  levels were probably high during non-glacial intervals [1]. Combined with other changes,  $\tau_s$  on the order of 10–100 My is conceivable.

The evidence for such a long relaxation time lies in the isotopic record. Perturbations to the carbon cycle at time scales much greater than  $\tau_s$  are quasi-static, simply shifting  $\varepsilon^*$  and  $\delta_a^*$ . However perturbations to  $\delta_a$  and  $\delta_o$  at time scales less than  $\tau_s$  but greater than  $\tau_1$  will result in trajectories parallel to the eigenvector  $\mathbf{v}_1$ . After transformation to the  $\varepsilon, \delta_a$  phase plane,  $\mathbf{v}_1$  has slope  $1 - \mu \simeq 1$ . Thus the slopes of unity seen in Figure 2 result from  $\mu \ll 1$ , which corresponds to  $\tau_2 = \tau_1/\mu \gtrsim 10^4$  yr.

In contrast, the average residence time for dissolved and particulate organic carbon (obtained from a mass-weighted sum of inverse residence times) in modern oceans is  $\tau_2 \simeq 40$  yr [14], yielding  $\mu \simeq 25$ . Presently  $j_{12} \simeq j_{21} \simeq J_1 \simeq J_2$ ; therefore  $m_2 \simeq m_1/\mu$ . Assuming similar relations held in the past and that  $m_1$  has not appreciably changed, we find that organic carbon in Neoproterozoic oceans must have been at least 2–3 orders of magnitude more abundant than at present and that its average age was similarly greater.

Evidently the organic-rich oceans were stratified, with oxygenated shallow waters overlying anoxic deep waters in which organic matter persisted. The redox stratification was maintained dynamically. Prior to the advent of biomineralization [17] and the evolution of planktonic animals that produced fecal pellets [18], organic material tended to remain in suspension. Any oxygen produced by photosynthesis that had not evaded to the atmosphere would have been consumed by respiration processes in surface waters, with the deep pool of organic matter acting as a buffer against deep ocean ventilation. (Consequently deep ocean sulfate concentrations would have also been suppressed [19].) Organic matter which escaped the euphotic zone could

have dissolved or aged through fermentative processes, but it otherwise was stored at depth. Upon upwelling, it could be remineralized, thereby suppressing rises in oxygen concentrations.

Modern oceans provide some supporting evidence. The age of dissolved organic carbon is presently about 5000 yrs [20], which is roughly similar to our lower bound for the Neoproterozoic remineralization time scale,  $\tau_2 \gtrsim 10^4$  yr. Thus Neoproterozoic dissolved organic carbon need not have been extraordinarily old compared to its modern counterpart. It was, however, the dominant form, with the result that  $\tau_2$  was vastly greater than at present. Studies of Neoproterozoic and older sedimentary organic matter may help to define its chemical form.

## Isotopic Events

As already indicated, there are two generic ways to drive the Neoproterozoic isotopic events: by changing the fluxes, or by changing the isotopic compositions they carry. The latter is best exemplified by variations in  $\varepsilon_0$ , and we consider it first.

The reality and potential importance of changes in  $\varepsilon_0$  are demonstrated by the Cenozoic record. Given the evidence (Figure 1a) that  $f$  was roughly constant and that the carbon cycle evolved through a sequence of steady states, we find  $\varepsilon_0 = \varepsilon$ . The Cenozoic variations in  $\varepsilon$  must therefore be ascribed to changes in levels of  $\text{CO}_2$ , abundances of nutrients that controlled rates of algal growth, and aspects of algal physiology such as cell-wall permeabilities and surface-to-volume ratios [21].

All else (i.e.,  $f$ , reservoir sizes, and fluxes) being constant, changes in  $\varepsilon_0$  at a rate  $\nu$  such that  $\tau_s^{-1} \lesssim \nu \lesssim \tau_1^{-1}$  will generate steeply sloped ( $\hat{f} \simeq 1$ ) trajectories provided that  $\mu \ll 1$ . We consider the positive excursion seen between 645 Ma and 594 Ma in Figure 2a as an example. Here  $\varepsilon$  rises and then falls by roughly 5‰. To provide a continuous function plausibly representing related variations in  $\varepsilon_0$ , we use

$$\varepsilon_0(t) = \bar{\varepsilon}_0 + a \sin(2\pi\nu t), \quad (15)$$

where we set  $\bar{\varepsilon}_0 = 28\text{‰}$ ,  $a = 5\text{‰}$ , and  $\nu = (10^5\tau_1)^{-1}$ . We then solve equations (6)–(9) numerically, using  $\delta_i = -6\text{‰}$ , specifying a normalized photosynthetic flux  $\phi_{12} \equiv j_{12}/J_1 = 0.999$ , and obtaining the normalized remineralization flux  $\phi_{21} = (\phi_{12} - f)/(1 - f) \simeq 0.999$  by choosing  $f = 0.3$ . Figure 4a compares the resulting theoretical trajectory, depicted here through approximately one-half cycle in  $\varepsilon_0$ 's variations, with observations. The control parameter  $\mu = 10^{-2}$ . If  $\tau_1 = 10^3$  yr is assumed, the parameter choices yield  $\tau_2 = 10^5$  yr,  $\tau_s \simeq 7 \times 10^7$  yr, and  $\varepsilon_0$  varying with a period of  $10^8$  yr. The comparison between theory and observations is remarkably good.

We next consider changes in fluxes. The large Neoproterozoic organic carbon reservoir suggests an enhanced remineralization flux  $j_{21}$  as a mechanism for driving negative isotopic events. A simple calculation shows how this could happen. Presently the oceans contain about  $3.2 \times 10^{18}$  moles of inorganic carbon [14]. The Neoproterozoic reservoir of organic carbon should have been at least ten times greater, i.e., at least

$32 \times 10^{18}$  moles of organic carbon. Now suppose we seek a 10‰ negative shift in  $\delta_a$ , from  $\delta_a = 5\text{‰}$  to  $\delta_a = -5\text{‰}$ , in an inorganic reservoir of modern size. Then if  $\delta_o = -25\text{‰}$ , we need only transfer  $1.6 \times 10^{18}$  moles of organic carbon, or at most 5% of the organic reservoir, to reservoir 1. Assuming each mole of remineralized organic carbon is oxidized by a mole of  $\text{O}_2$ , such a transfer would require  $1.6 \times 10^{18}$  moles  $\text{O}_2$ . The present-day atmosphere contains roughly  $37 \times 10^{18}$  moles  $\text{O}_2$  [22]. Thus only about 4% of the present atmospheric inventory of oxygen would be required.

As an example, we consider the negative excursion in Figure 2a between 583 Ma and 555 Ma. We use the same parameter choices as detailed above, but fix  $\varepsilon_0 = \bar{\varepsilon}$  and let  $\phi_{21}$  vary like

$$\phi_{21}(t) = \phi_{21}^{(0)} + a(1 - \cos(2\pi\nu t))/2 \quad (16)$$

for  $0 \leq \nu t \leq 1$ , with  $\phi_{21}^{(0)}$  equal to the value of  $\phi_{21}$  used above,  $a = 0.23$ , and  $\nu = 0.03$ . Comparison of theory to data is shown in Figure 4b. If we again assume  $\tau_1 \simeq 10^3$  yr, the time scale of the theoretical trajectory is  $\tau_1/\nu \simeq 3 \times 10^4$  yr. The theoretical and observed trajectories compare well, but the time scales are different. Note, however, that longer time scales are possible: numerical solutions show that the trajectory in Figure 4b is qualitatively invariant for  $\nu \simeq \mu \ll 1$ .

Such issues of timing are likely to evolve as the Neoproterozoic time scale itself evolves [23]. Although details of our interpretations may change as new absolute dates are obtained, we expect that the overall validity of our model will be insensitive to such revisions.

## Discussion and Conclusion

We have thus far deduced the following: *i*) the Neoproterozoic carbon cycle evolved dynamically, out of steady state; *ii*) the lack of a steady state was due to a large oceanic reservoir of organic carbon; and *iii*) the large organic reservoir led to large fluctuations in  $\delta_a$ , either passively, via changes in  $\varepsilon_0$ , or actively, via temporarily enhanced remineralization. Consideration of pertinent records may well show that the same processes were important at earlier times.

The isotopic records at present cannot distinguish between the passive and active mechanisms. The different senses of rotation in Figures 4a and 4b could help, but remaining geochronological uncertainties and noise in the records probably render inferences statistically insignificant. The fact that changes in  $\varepsilon_0$  require longer relaxation times may also be useful, but better estimates of  $\tau_1$  and  $\mu$  and improved geochronology would be required for a definitive conclusion. Isotopic analyses of biomarkers related to photosynthetic pigments, algal sterols, or cyanobacterial hopanoids can indicate variations in the isotopic composition of primary products. These may provide a tool for showing that changes in  $\varepsilon$  result from changes in  $\varepsilon_0$ .

Any further interpretation of the isotopic events must of course take into account known environmental changes. Hoffman and Schrag [9] have assembled compelling evidence indicating that apparently fast, deep ( $\gtrsim 10\text{‰}$ ) declines in the Neoproterozoic

$\delta_a$  record were accompanied by major glaciations of possibly global extent—a “snow-ball Earth.” The duration of one or more of these negative excursions may have been as short as  $6 \times 10^5$  yr [24]. Such a fast event would be difficult to reconcile with large changes in  $\varepsilon_0$ . However it is easily accommodated by a temporary increase in  $j_{21}$ . What, then, would have triggered the enhanced oxidation of the organic reservoir?

More  $O_2$  would be partitioned into the ocean in a colder climate. The solubility of  $O_2$  nearly doubles as seawater cools from  $30^\circ\text{C}$  to  $0^\circ\text{C}$ . Although low temperatures would decrease biological activity,  $O_2$  would be present, and aerobic respiration possible, in a greater portion of the ocean. The effect would be amplified by enhanced convective circulation. Overall rates of remineralization would increase and  $\delta_a$  would decline.

Concurrent with  $\delta_a$ 's decline would be an increase in  $CO_2$  levels resulting from the increased oxidation of organic carbon. These changes would have been most significant at low latitudes, where the decrease in temperature due to advancing ice sheets and the surface area over which the change occurred would have been greatest. The attendant atmospheric greenhouse effect might then have acted to arrest the glaciation. The “white Earth” instability [25] may have therefore not been fully realizable. Glaciations may have advanced near, but not entirely to, the equator [26].

The terminal Proterozoic negative isotopic excursion [3–5] requires a different interpretation. First, no associations with glaciations have been found [27]. Second, its representation in Figure 1b is consistent with quasi-static rather than dynamic evolution.

The final event is correlated with a dramatic change in isotopic relationships between biomarkers representing primary producers and consumers. That signal has been interpreted as marking the advent of rapidly sinking particulate organic carbon, specifically fecal pellets [18]. Although packaging and hydrodynamic factors alone are not insignificant, the requirement that sinking particles include some dense, inorganic ballast is more important [28]. Accordingly, the isotopic change may indicate *i*) that fecal pellets produced by the first planktonic animals with guts significantly enhanced the combination of organic material with lithogenic debris and/or with calcium carbonate from whittings; *ii*) the radiation of algae containing resistant biopolymers in cell walls and cysts [29,30]; or *iii*) the development of biomineralization [17].

More broadly, the earlier work postulated linkages between the accelerated removal of organic material from surface waters, the ventilation of ocean depths, and the rise of  $O_2$  [18]. To those events is now added the demise of a large reservoir of long-lived organic carbon suspended in seawater. In this view, the  $^{13}\text{C}$ -enriched secondary biomarkers would have been products of that reservoir and the bacterial processes associated with it. Redox buffering of the deep ocean by sulfide [19] was supplemented by, or perhaps even secondary to, the effects of the large pool of suspended organic carbon. The interactions inherent in this system lead naturally to the coincidence of three independent isotopic signals: the onset of quasi-static evolution of the carbon-isotopic records (Figure 1b) and the negative excursion accompanying it [3–5]; the disappearance of  $^{13}\text{C}$ -enriched secondary biomarkers [18]; and the onset

of complementarity between the isotopic records of carbonate carbon and oceanic sulfate [31,32]. Further correspondences are likely to be found.

We thank S. Bowring and H. Hartman for helpful discussions, and D. Des Marais, A. Knoll, and L. Kump for timely and critical reviews of the manuscript. This work was supported in part by NSF Grant DEB-0083983, NASA Exobiology Grant NRA-01-01-EXB-006, and NASA Astrobiology Institute Grant NCC2-1053.

## References

- [1] Des Marais, D. J. (1997) in *Geomicrobiology: Interactions between microbes and minerals*, eds. Banfield, J. F & Nealson, K. H. (Mineralogical Society of America, Washington, D. C.), pp. 429–448.
- [2] Freeman, K. H. (2001) in *Stable Isotope Geochemistry*, eds. Valley, J. W & Cole, D. R. (Mineralogical Society of America, Washington, D. C.), pp. 589–606.
- [3] Magaritz, M, Holser, W. T, & Kirschvink, J. L. (1986) *Nature* **320**, 258–259.
- [4] Kimura, H, Matsumoto, R, Kakuwa, Y, Hamdi, B, & Zibaseresht, H. (1997) *Earth and Planetary Science Letters* **147**, E1–E7.
- [5] Bartley, J. K, Pope, M, Knoll, A. H, Semikhatov, M. A, & Petrov, P. Y. (1998) *Geol. Mag.* **135**, 473–494.
- [6] Knoll, A. H, Hayes, J. M, Kaufman, A. J, Swett, K, & Lambert, I. B. (1986) *Nature* **321**, 832–838.
- [7] Knoll, A. H, Bambach, R. K, Canfield, D. E, & Grotzinger, J. P. (1996) *Science* **273**, 452–457.
- [8] Hoffman, P. F, Kaufman, A. J, Halverson, G. P, & Schrag, D. P. (1998) *Science* **281**, 1342–1346.
- [9] Hoffman, P. F & Schrag, D. P. (2002) *Terra Nova* **14**, 129–155.
- [10] Knoll, A. H & Carroll, S. B. (1999) *Science* **284**, 2129–2137.
- [11] Bergé, P, Pomeau, Y, & Vidal, C. (1984) *Order within Chaos: Towards a Deterministic Approach to Turbulence*. (John Wiley and Sons, New York).
- [12] Kump, L. R & Arthur, M. A. (1999) *Chemical Geology* **161**, 181–198.
- [13] Holland, H. D. (1978) *The Chemistry of the Atmosphere and Oceans*. (John Wiley & Sons, New York).

- [14] Holser, W. T, Schidlowski, M, Mackenzie, F. T, & Maynard, J. B. (1988) in *Chemical cycles in the evolution of the Earth*, eds. Gregor, C. B, Garrels, R. M, Mackenzie, F. T, & Maynard, J. B. (John Wiley & Sons, New York), pp. 105–173.
- [15] Hayes, J. M, Strauss, H, & Kaufman, A. J. (1999) *Chemical Geology* **161**, 103–125.
- [16] Rayner, J. M. V. (1985) *J. Zool., Lond. (A)* **206**, 415–439.
- [17] Lowenstam, H. A & Weiner, S. (1989) *On Biomineralization*. (Oxford University Press, New York).
- [18] Logan, G. A, Hayes, J. M, Hieshima, G. B, & Summons, R. E. (1995) *Nature* **376**, 53–536.
- [19] Canfield, D. E. (1998) *Nature* **396**, 450–453.
- [20] Druffel, E. R. M, Williams, P. M, Bauer, J. E, & Ertel, J. R. (1992) *Journal of Geophysical Research* **97**, 15639–15659.
- [21] Popp, B. N, Laws, E. A, Bidigare, R. R, Dore, J. E, Hanson, K. L, & Wakeham, S. G. (1998) *Geochimica and Cosmochimica Acta* **62**, 69–77.
- [22] Keeling, R. F, Najjar, R. P, Bender, M. L, & Tans, P. P. (1993) *Global Biogeochemical Cycles* **7**, 37–67.
- [23] Walter, M. R, Veevers, J. J, Calver, C. R, Gorjan, P, & Hill, A. C. (2000) *Precambrian Research* **100**, 371–433.
- [24] Halverson, G. P, Hoffman, P. F, Schrag, D. P, & Kaufman, A. J. (2002) *Geochemistry Geophysics Geosystems* **3**, art. no. 1035.
- [25] Budyko, M. I. (1977) *Climatic Changes*. (American Geophysical Union, Washington, D.C.).
- [26] Hyde, W. T, Crowley, T. J, Baum, S. K, & Peltier, W. R. (2000) *Nature* **405**, 425–429.
- [27] Kaufman, A. J, Knoll, A. H, & Narbonne, G. M. (1997) *Proc. Natl. Acad. Sci. USA* **94**, 6600–6605.
- [28] Francois, R, Honjo, S, Krishfield, R, & Manganini, S. (2002) *Global Biogeochemical Cycles* **16**, art. no. 1087.
- [29] Zang, W. L & Walter, M. R. (1989) *Nature* **337**, 642–645.
- [30] Derenne, S, Leberre, F, Largeau, C, Hatcher, P, Connan, J, & Raynaud, J. F. (1992) *Organic Geochemistry* **19**, 345–350.

- [31] Veizer, J, Holser, W. T, & Wilgus, C. K. (1980) *Geochim. Cosmochim. Acta* **444**, 579–587.
- [32] Hayes, J. M, Lambert, I. B, & Strauss, H. (1992) in *The Proterozoic Biosphere, a Multidisciplinary Study*, eds. Schopf, J. W & Klein, C. (Cambridge University Press, Cambridge), pp. 129–132.
- [33] Efron, B & Tibshirani, R. J. (1993) *An Introduction to the Bootstrap*. (Chapman and Hall/CRC, New York).

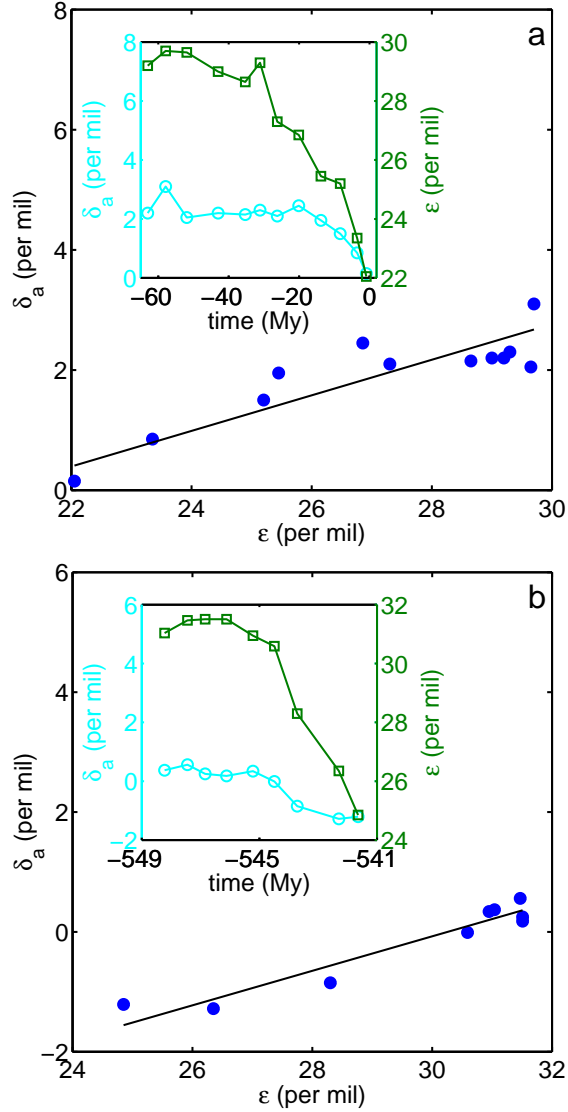


Figure 1: (a) The isotopic content of carbonate carbon ( $\delta_a$ ) versus the fractionation between carbonate and marine organic carbon ( $\varepsilon$ ) for the Cenozoic, along with the best-fitting straight line (the reduced major axis [16]). The line's slope is  $\hat{f} = 0.30$ , with 95% confidence interval [0.18, 0.36]; its intercept is  $\hat{\delta}_i = -6.1\text{‰}$  [ $-7.6\text{‰}$ ,  $-2.8\text{‰}$ ] ( $r = 0.88$ ,  $n = 12$ ). Confidence intervals are computed using the bootstrap method [33]. Inset: the time dependence of  $\delta_a$  (cyan  $\circ$ ) and  $\varepsilon$  (green  $\square$ ). (b) The same analysis for a more highly resolved period in the latest Precambrian and early Cambrian, resulting in  $\hat{f} = 0.29$  [0.23, 0.43] and  $\hat{\delta}_i = -8.7\text{‰}$  [ $-13.2\text{‰}$ ,  $-7.1\text{‰}$ ] ( $r = 0.96$ ,  $n = 9$ ). The data, from Ref. [15], are computed from global averages. The average standard deviations of these mean values are  $0.3\text{‰}$  ( $\delta_a$ ) and  $0.9\text{‰}$  ( $\varepsilon$ ) in (a) and  $0.1\text{‰}$  ( $\delta_a$ ) and  $0.8\text{‰}$  ( $\varepsilon$ ) in (b).

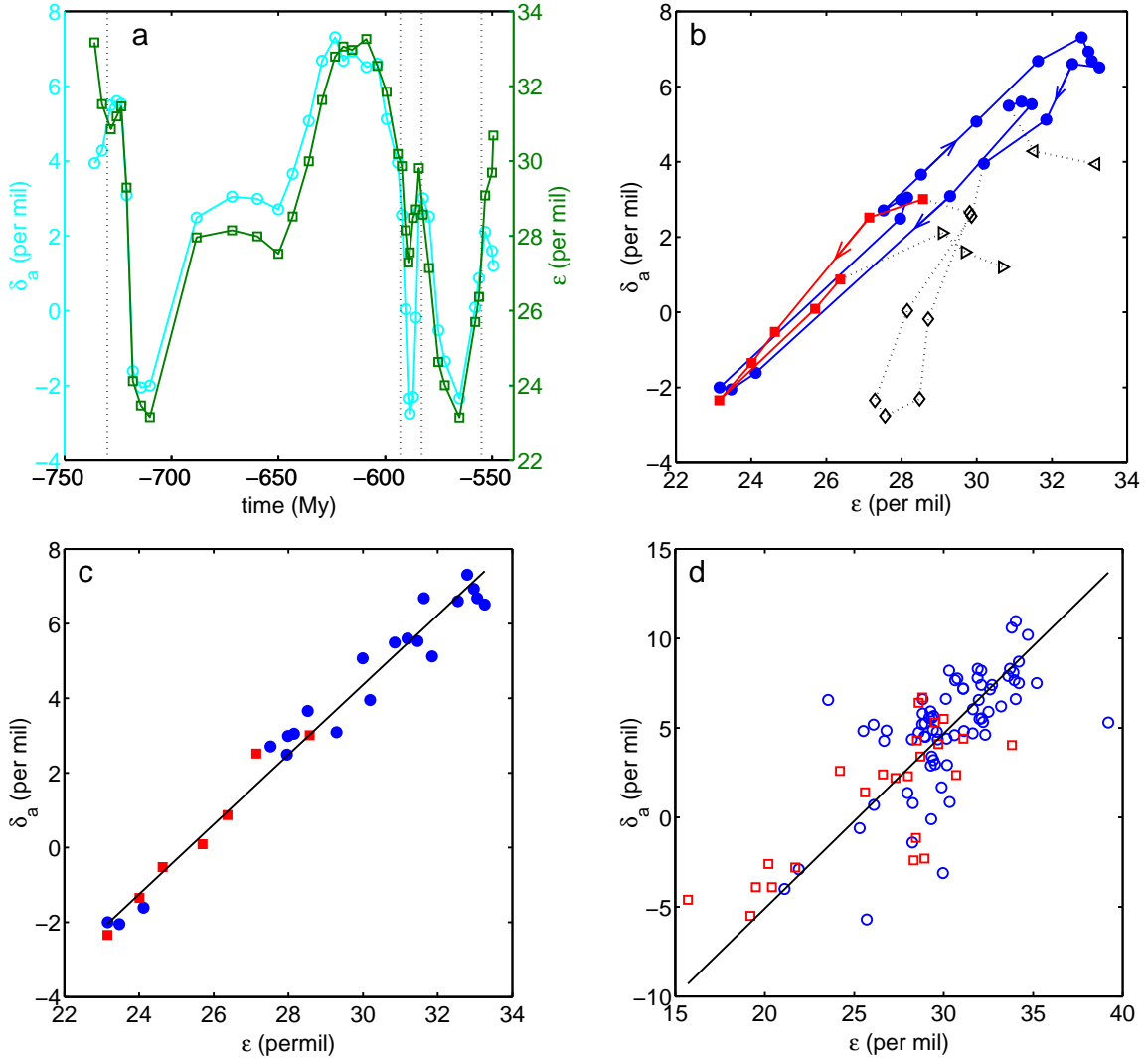


Figure 2: (a) Time dependence of  $\delta_a$  (cyan  $\circ$ ) and  $\varepsilon$  (green  $\square$ ) in the Neoproterozoic, computed from global averages [15]; the mean standard deviations are  $0.6\text{‰}$  ( $\delta_a$ ) and  $1.0\text{‰}$  ( $\varepsilon$ ). Dotted lines correspond to  $t = -730, -593, -583,$  and  $-555$  Ma. (b) Corresponding trajectories in the  $\varepsilon - \delta_a$  phase plane; arrows indicate the direction of time. Symbols correspond to the following time intervals:  $\triangleleft$ , 738–730 Ma; blue  $\bullet$ , 730–593 Ma;  $\diamond$ , 593–583 Ma; red  $\blacksquare$ , 583–555 Ma;  $\triangleright$ , 555–549 Ma. (c) The data from (b) corresponding only to its blue and red intervals, compared to the best-fitting straight line. The slope  $\hat{f} = 0.94$  [0.88, 0.98] and the intercept  $\hat{\delta}_i = -23.7\text{‰}$  [ $-25.0\text{‰}, -22.2\text{‰}$ ] ( $r = 0.99, n = 28$ ). (d) The complete set of unaveraged  $\varepsilon - \delta_a$  pairs that occur within the same rock sample and contribute to the mean values plotted in (c), compared to the best-fitting straight line. The slope  $\hat{f} = 0.98$  [0.85, 1.15] and the intercept  $\hat{\delta}_i = -24.6\text{‰}$  [ $-30.0\text{‰}, -20.7\text{‰}$ ] ( $r = 0.76, n = 98$ ). Time intervals: blue  $\circ$ , 731–590 Ma; red  $\square$ , 583–553 Ma.

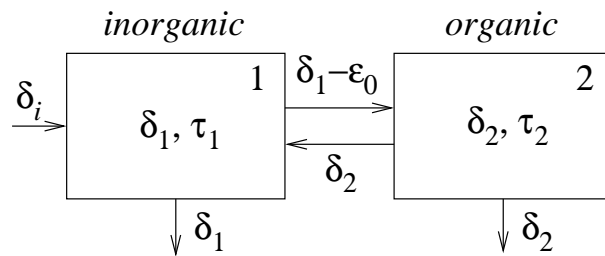


Figure 3: A carbon-cycle model with two time scales,  $\tau_1$  and  $\tau_2$ . Reservoir 1 denotes the oceans' inorganic carbon, with isotopic content  $\delta_1$ ; reservoir 2 denotes organic carbon, with isotopic content  $\delta_2$ . Fluxes between reservoirs represent photosynthesis (including isotopic depletion by an amount  $\epsilon_0$ ) and remineralization; fluxes out of the reservoirs represent burial. The flux into reservoir 1 represents volcanic and other inputs with isotopic content  $\delta_i$ .

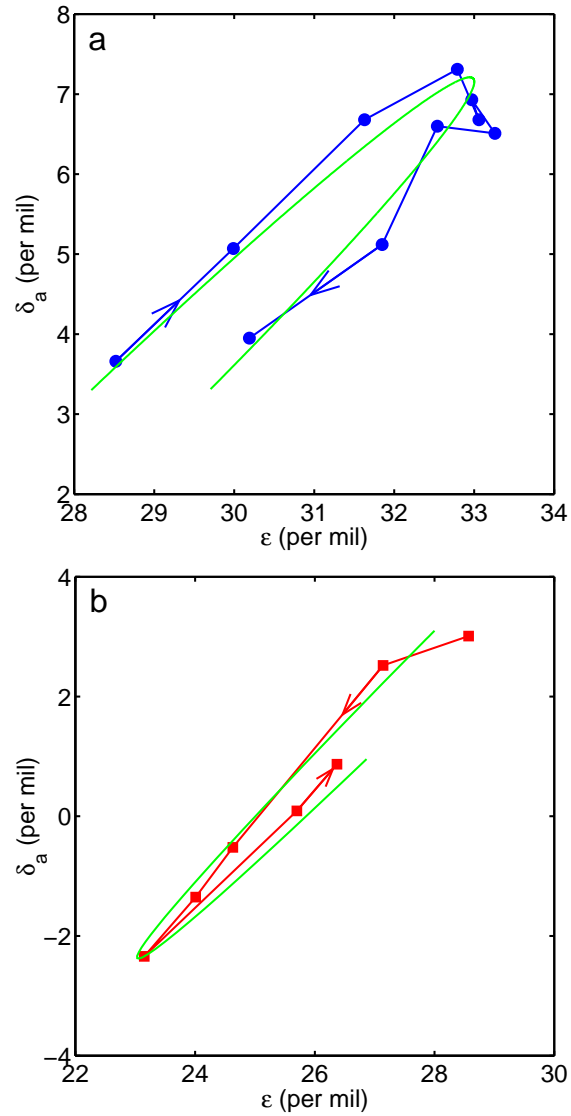


Figure 4: Neoproterozoic observations compared to theory. (a) The positive excursion between 645 Ma and 594 Ma (blue circles; compare to Figures 2a and 2b) compared to approximately one-half cycle in the evolution of equations (6)–(9) (smooth green line), with  $\epsilon_0$  varying according to equation (15). The control parameter  $\mu = 10^{-2}$ . Both trajectories flow in the same clockwise direction. (b) The negative excursion between 583 Ma and 555 Ma (red squares; compare to Figures 2a and 2b) compared to theory (smooth green line), where now  $\epsilon_0$  is constant but the remineralization flux varies according to equation (16). Once again  $\mu = 10^{-2}$ . Both trajectories flow in the counter-clockwise direction.